Proceedings of the Zoological Institute RAS
Vol. 323, No. 3, 2019, pp. 347–363
10.31610/trudyzin/2019.323.3.347

УДК 599.363

Comparative analysis of shrew tooth pigmentation using energy-dispersive X-ray spectroscopy (EDX)

L.L. Voyta[1]*, V.S. Zazhigin[2] and A.A. Miroljubov[1]

[1]*Zoological Institute, Russian Academy of Sciences, Universitetskaya nab. 1, Saint Petersburg, 199034, Russia;*
e-mails: leonid.voyta@zin.ru; alexei.miroljubov@zin.ru

[2]*Geological Institute, Russian Academy of Sciences, Pyzhevskii per. 7, Moscow, 109017, Russia; e-mail: zazhvol@gmail.com*

ABSTRACT

The pigment of tooth enamel is an important odontological character for character for assessing Soricidae taxonomy and phylogeny. This paper describes the original observations of ‘pigment patterns’ (PPt) and ‘visible pigment’ (VPg) in fossil beremendiin shrews in light of the “differential pigmentation” found using UV detection and EDX analysis. The term “differential pigmentation” was used to describe the irregular pigmentation on the teeth of extinct *Nesiotites* (Neomyini). Our analysis of fossil and recent specimens reveals different reasons for differential pigmentation formation. The first reason is related to fossilization, namely, the chemical alterations of the buried specimen. The second reason is related to a developmental disorder, namely, the enamel organ disorder, which locally stops forming the twin enamel layer. Our original results and published data from EDX analysis of the enamel elemental content and SEM-image analysis of the enamel microstructure again raise the question of a relationship between ferruginous pigmentation and enamel microstructure. Further studies of the enamel structure and pigment chemical composition of red-toothed shrews compared to white-toothed shrews are required.

Key words: *Anourosorex*, *Beremendia*, EDX analysis, enamel pigmentation, red-toothed shrews, *Sorex*, Soricinae

Сравнительный анализ пигментации зубов землероек с использованием энергодисперсионной рентгеновской спектроскопии (EDX)

Л.Л. Войта[1]*, В.С. Зажигин[2] и А.А. Миролюбов[1]

[1]*Зоологический институт Российской академии наук, Университетская наб. 1, 199034 Санкт-Петербург, Россия; e-mail: leonid.voyta@zin.ru; alexei.miroljubov@zin.ru*

[2]*Геологический институт Российской академии наук, Пыжевский пер. 7, 109017 Москва, Россия;*
e-mail: zazhvol@gmail.com

РЕЗЮМЕ

Пигментация зубной эмали является важным одонтологическим признаком для разработки таксономии и филогении Soricidae. В статье описываются оригинальные наблюдения «пигментных пятен» (PPt) и «видимого пигмента» (VPg) у ископаемых беремендий в связи с вопросом о «дифференциальной пигментации». В работе были использованы метод УФ-детекции пигмента и EDX-анализ. Термин «дифференциальная пигментация» использовался для объяснения неоднородной пигментации на зубах вымерших *Nesiotites* (Neomyini). Наш анализ ископаемых и современных экземпляров выявил некоторые причины проявления дифференциальной пигментации. Первая причина связана с

---

* *Corresponding author / Автор-корреспондент*

условиями захоронения, а именно с химическими изменениями погребенного объекта. Вторая причина связана с нарушением развития, а именно с нарушениями в работе эмалевого органа, который локально ограничивает формирование двойного слоя эмали. Наши результаты и опубликованные данные EDX-анализа элементного состава эмали и анализа микроструктуры эмали с применением SEM вновь ставят вопрос о соответствии железосодержащей пигментации и микроструктуры эмали. Требуются дальнейшие исследования структуры эмали и химического состава пигмента у бурозубковых в сравнении с белозубковыми землеройками.

Key words: *Anourosorex*, *Beremendia*, EDX-анализ, пигментация эмали, бурозубковые землеройки, *Sorex*, Soricinae

---

INTRODUCTION

Reddish colouration of the teeth is an important characteristic in the definition of the subfamilies of Soricidae Fischer, 1817. Tooth pigmentation is known in the Heterosoricinae Viret and Zapfe, 1951, Limnoecinae Repenning, 1967, Crocidosoricinae Reumer, 1987 and Soricinae Fischer, 1817. However, it is not found in Soricolestinae Lopatin, 2002, Allosoricinae Fejfar, 1966 and Crocidurinae Milne-Edwards, 1868 (Repenning 1967; Reumer 1994; Dannelid 1998; Lopatin 2002).

It is assumed that the iron in shrew teeth enamel makes it harder and generally increases the wear resistance of teeth (Janis and Fortelius 1988; Jernvall 1995). According to the most recent study of enamel pigment (Dumont et al. 2014), the structurally red colouration of soricine teeth (*Blarina brevicauda* (Say, 1823) was examined) is based on "[...] an ultrafine-grained magnetite phase [which] is distributed around the hydroxyapatite crystals [...]" (Dumont et al. 2014: 47). The authors show that the pigmented enamel is harder than unpigmented enamel. Despite this evidence, the exact reason for the iron inclusions is still unclear, but it is probable that pigmented enamel is more resistant to acid or to mechanical loads (*ibid.*).

Among extant soricine taxa, the intensity of the tooth colouration varies widely, from invisible to the naked eye (e.g., the phenomenon known in *Anourosorex* Milne-Edwards, 1872; *Chimarrogale* Anderson, 1877; and *Nectogale* Milne-Edwards, 1870) to very dark pigmented teeth (*Beremendia* Kormos, 1930; *Blarina* Gray, 1837; *Blarinella* Thomas, 1911). All species of the genus *Sorex* Linnaeus, 1758, have pigmented teeth with different degrees of colouration, from light orange in *S. minutus* Linnaeus, 1766, to different shades of red in most species, to deeply dark in *S. daphaenodon* Thomas, 1907. However, the extinct taxa display unclear colouration that is very often associated with burial conditions (e.g., the chemical composition of sediments, groundwaters and others). The tooth pigment patterns and their intensity of colouration would be useful for taxonomic and phylogenetic analyses of fossil groups. However, in many cases, researchers refuse to use the teeth colouration due to the inability to assess the impact of burial conditions and distinguish the nature of 'pigment patterns' (PPt) and 'visible pigment' (VPg). For instance, the so-called "differential pigmentation" of extinct shrews *Nesiotites* Bate, 1944, contributes the argument disputing the validity of "*Nesiotites rafelinensis*" (Rofes et al. 2012; Furió and Pons-Monjo 2013). The precise description of a neotype of *Miosorex desnoyersianus* (Lartet, 1851) by Engesser (2009: 21) points to tooth pigmentation; in contrast, descriptions of mass material of *Miosorex pusilliformis* (Doben-Florin, 1964) and *M. desnoyersianus* by Doben-Florin (1964) and Ziegler (1989) do not confirm differential pigmentation of their teeth. If *Miosorex* s. lato (European *Miosorex* Kretzoi, 1959, + Asian *Shargainosorex* Zazhigin et Voyta, 2018) should be considered as an ancestral group to recent shrew groups, pigmentation is a significant feature for determining phylogenetic relations. Therefore, a means for pigment diagnostics is needed. One of the precise methods for pigment detection is energy-dispersive X-ray spectroscopic (EDX) analysis, which was first used for ferruginous teeth pigment detection in shrews by Dötsch and Koenigswald (1978). The current literature describes the elemental composition of the enamel pigment of shrews using EDX (Dumont et al. 2014; Moya-Costa et al. 2018). Our paper describes the first observations of 'pigment patterns' (PPt) and 'visible pigment' (VPg) in fossil beremendiins in light of the "differential pigmentation" (see above). The primary objective of our work is to detect iron and quantitatively assess iron presence in fossil teeth from different localities in comparison with several recent taxa.

GEOLOGICAL AND GEOGRAPHICAL SETTINGS

The fossil material of *Beremendia fissidens* (Petényi, 1864) and *B. minor* Rzebik-Kowalska, 1976, come from five early Pliocene to Early Pleistocene sites in southwestern Siberia, northern Mongolia and the Russian Plain: Korotoyak 2 (KRK/2), Razdol'e (RZD), 'Borehole #103/19' (BH-103/19), Bural-Obo (BRB/C), and Shamar (SHM/A). These localities are mentioned in Agadjanian (2009), Vasilyan et al. (2017), Zazhigin and Voyta (2019). Below, the fossil sites are briefly described.

Korotoyak 2 (KRK/2). The geological profile is located on the right bank of the Don River, near Korotoyak village, Ostrogozhskii District, Voronezhskaya Oblast, Russia [ca. N 50°59´ E 039°10´]. The fossiliferous sediments were attributed to the late Pliocene, MN 16. Uryv formation. Material was collected by Yulia I. Iosifova in 1989–90 (Agadjanian 2009).

Razdol'e (RZD). The geological profile is located on the right bank of the Aley River (left tributary of Ob' river) after the mouth of the Kizikha River and situated between Makhanovo and Bolshevik (= Razdol'e) villages, Pospelikhinskii District, Altayskii Kray, Russia [ca. N 51°49´ E 081°45´]. The fossiliferous sediments were attributed to the Early Pleistocene (the first half of the Calabrian). The formation was undetermined. Material was collected by Vladimir S. Zazhigin in 1965 (Zazhigin 1980).

'Borehole #103/19' (BH-103/19). The analysed sample with beremendiin remains was found in the kern of borehole #103/19 (approximately 70–78 m deep) near Troitskoye (Troinka) village Pospelikhinskii District, Altayskii Kray, Russia [ca. N 51°32´ E 081°38´]. Both the geological age of redeposited fossiliferous sediments and their attribution to particular formation remain undetermined. Material was collected by Oleg M. Adamenko and Yurii M. Kolikhalov, years unknown (Zazhigin 1980).

Bural-Obo (BRB/C). The geological profile is located on the right bank of the Orkhon River (right tributary of the Selenga River), 2 km west of Bural-Obo Rock in an old brick quarry, approximately 6 km upstream of the river from Shamar village, Selenge Aimag, Mongolia [ca. N 50°02´ E 106°08´]. The fossiliferous sediments were attributed to the Early Pleistocene, MN 17. The formation was undetermined. Material was collected by Vladimir S. Zazhigin in 1970 (Devyatkin and Zazhigin 1974; Devjatkin et al. 1982; Zazhigin 1989).

Shamar (SHM/A). The geological profile is located on the left bank of the Orkhon River on the northern slope of the Ikh-Burge Rock in the artificial hollow for an electric transmission tower, 2 km west of Shamar village, Selenge Aimag, Mongolia [ca. N 50°03´ E 106°07´]. The fossiliferous sediments were attributed to the late Pliocene, MN 16. Chikoy formation. Material was collected by Vladimir S. Zazhigin in 1970 (Devyatkin and Zazhigin 1974; Devjatkin et al. 1982; Zazhigin 1989).

MATERIALS AND METHODS

In order to detect the ferriferous pigment of teeth, energy-dispersive X-ray spectroscopy (EDX) was used. EDX represents a method for the elemental analysis or determination of the chemical composition of a sample (for a more detailed description of the technique used for shrew teeth, see Strait and Smith 2006). The EDX-spectrometer was attached to an electron microscope, Zeiss ESEM Quanta 250. Its technical specifications were as follow: quantification method = normalized stoichiometry; accelerating voltage = 15 kV; acquisition time = 30 s. Quantitative microanalyses were carried out on the surface of the teeth on a pigmented and unpigmented part of the crown. The values of the iron content was analysed in fossil specimens of *B. fissidens* – ZIN 104903/1292 (GIN 959/1292; isolated first upper right incisor from Korotoyak 2); ZIN104908/1236 (GIN 959/1236; isolated first upper left incisor from Shamar/A); GIN 664/201 (ZIN 104896; right dentary of *Nectogalinia altaica* Gureev, 1979 holotype from Razdol'e); ZIN 104925/1271 (GIN 959/1271; isolated first upper right molar form 'Borehole #103/19'); in fossil specimen of *B. minor* – ZIN 104894 (GIN 959/1242; right dentary from Bural-Obo/C); in extant specimens of *Sorex isodon* Turov, 1924 (field number 201/A86), *Crocidura shantungensis* Miller, 1901 – ZIN 89478 (Far East, Russia) and *Anourosorex squamipes* Milne-Edwards, 1872 – ZIN 38946 (South China). The results of the EDX analyses represented the averaged (mean) elemental composition (Weight %)

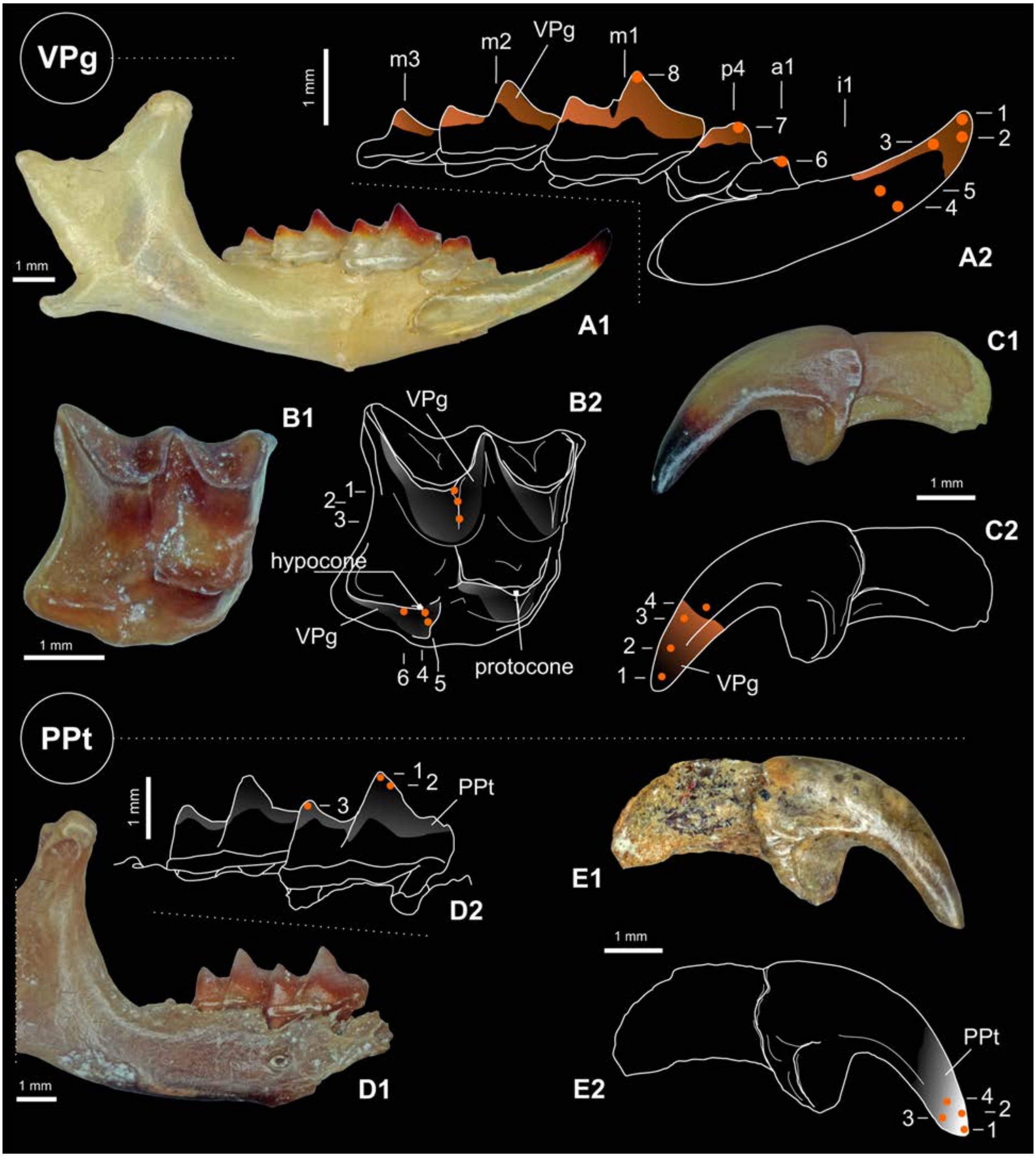

Fig. 1. *Beremendia minor* (A) and *B. fissidens* (B–E) fossil remains: **(A1)** Right dentary from Bural-Obo/C (ZIN 104894), optic photograph, lateral view; **(A2)** Explanatory drawing of lower dentition with VPg; **(B1)** First upper right molar from 'Borehole #103/19' (ZIN 104925/1271), optic photograph, occlusal view; **(B2)** Explanatory drawing of M1 with VPg; (C1) First upper left incisor from Shamar/A (ZIN104908/1236), optic photograph, lateral view; **(C2)** Explanatory drawing of I1 with VPg; **(D1)** Fragment of right dentary from Razdol'e (GIN 664/201), optic photograph, lateral view; **(D2)** Explanatory drawing of m1–m2 with PPt; **(E1)** First upper right incisor from Korotoyak 2 (ZIN 104903/1292) optic photograph, lateral view; **(E2)** Explanatory drawing of I1 with PPt. All scale bars represent 1 mm. Abbreviations: i1–m3 – lower dentition; orange points – the acquisition points of elemental analysis (numbers correspond to sample numbers in Tables 1 and 2); PPt – pigment pattern; VPg – visible pigment.

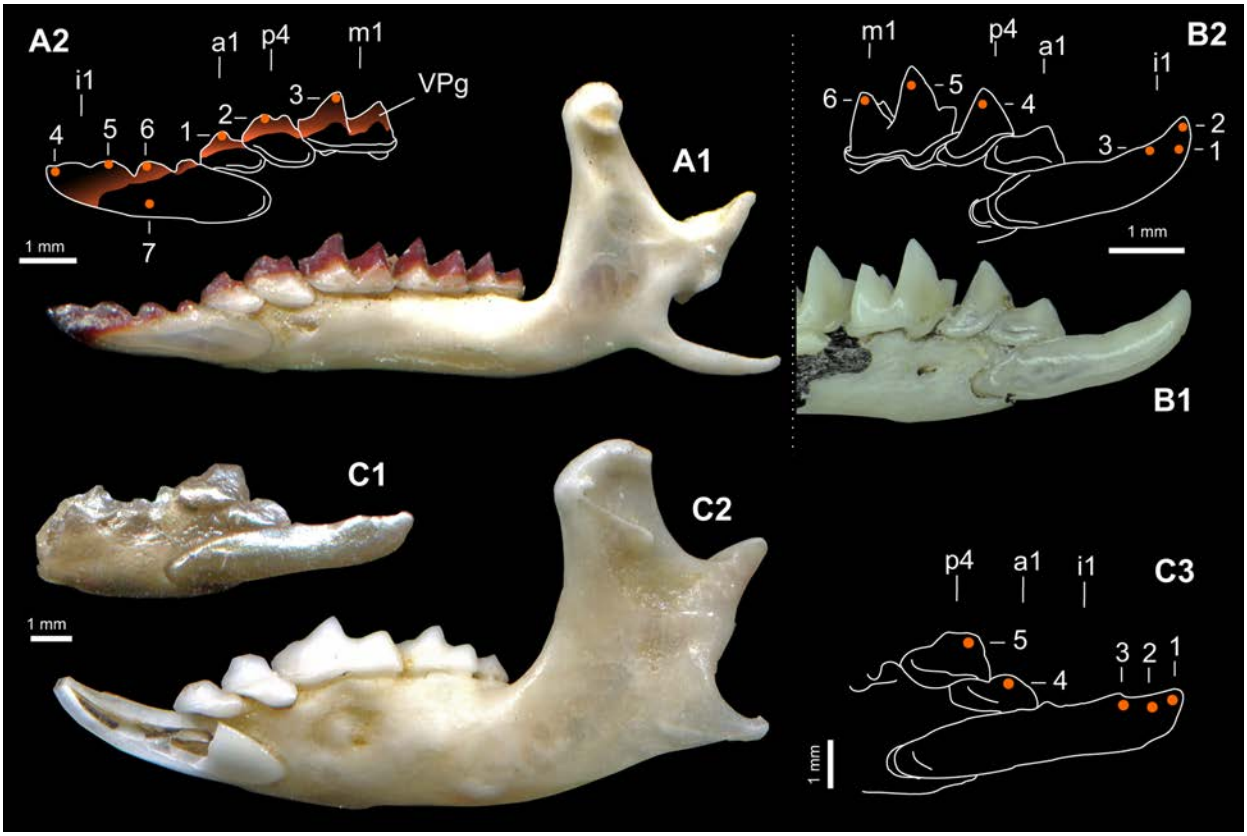

Fig. 2. *Sorex isodon* (A), *Crocidura shantungensis* (B) and *Anourosorex squamipes* (C) dentaries: (**A1**) Left dentary (201/A86), optic photograph, lateral view; (**A2**) Explanatory drawing i1–m1 with VPg; (**B1**) Fragment of right dentary (ZIN 89478), optic photograph, lateral view; (**B2**) Explanatory drawing i1–m1 without pigment; (**C1**) Fragment of right dentary with i1–p4 (ZIN 38946), optic photograph, lateral view; (**C2**) Left dentary with whole lower dentition, optic photograph, lateral view; (C3) Explanatory drawing i1–p4 without pigment. All scale bars represent 1 mm. Abbreviations see in Fig. 1.

normalized to 100%, with values of standard deviation (σ, Weight %). EDX analyses were performed using equipment of the «Taxon» Research Resource Center (http://www.ckp-rf.ru/ckp/3038/) of the Zoological Institute of the Russian Academy of Sciences (Saint Petersburg, Russia). The preliminary analyses were performed using the scanning electron microscope Hitachi TM3000 in the Resource Centre «Microscopy and Microanalysis» of Research park of Saint Petersburg State University (Saint Petersburg, Russia).

To register tooth pigment, a Zeiss AxioImager. A1 Zeiss Hbo 50/ac Fluorescence Mercury Light Source W Filter Set 49 microscope (Item Number 488049-9901-000; wavelength approximately 365–395 nm) was used for fluorescence applications, and a high-resolution AxioCam MRc 5 digital camera was used for image acquisition. Specimens were studied in transmitted UV light. The teeth were investigated at the Centre of Fluorescence Microscopy Facility of the Botanic Institute of the Russian Academy of Sciences (Saint Petersburg, Russia).

High-resolution images of the enamel microstructure were acquired using an electronic scanning microscope (Zeiss ESEM Quanta 250), with the surfaces covered by platinum sputter coating. SEM analyses of the enamel microstructure were performed on the etched (6–7% HCl for approximately 7–8 s) teeth following washing with distilled water.

RESULTS

The results of the analysis of fossil remains revealed the teeth had visible pigment (VPg) from red-

Table 1. Results of the EDX elemental analyses of the fossil teeth of *Beremendia*.

Sample number*	Tooth (pigmentation type)	Weight %	σ, Weight %	Element (Formula)
A: *B. minor* (ZIN 104894, Bural-Obo/C); Fig. 1A				
1	Tip of right i1 (VPg = black)	36.055	0.397	Oxygen
		15.077	0.260	Phosphorus (P2O5)
		22.945	0.299	Calcium (CaO)
		25.922	0.456	Iron (FeO)
2	Tip of right i1 (VPg = reddish)	20.703	0.279	Carbon (CO2)
		64.901	0.294	Oxygen
		4.629	0.071	Phosphorus (P2O5)
		8.616	0.097	Calcium (CaO)
		1.152	0.075	Iron (FeO)
3	Tip of right i1 (VPg = red-brown)	41.502	0.314	Oxygen
		0.500	0.104	Magnesium (MgO)
		1.128	0.102	Silicon (SiO2)
		19.946	0.233	Phosphorus (P2O5)
		31.516	0.273	Calcium (CaO)
		5.407	0.265	Iron (FeO)
4	Unpigmented distal part of i1 (white)	45.059	2.816	Oxygen
		13.331	1.762	Silicon (SiO2)
		14.864	2.191	Phosphorus (P2O5)
		26.746	2.450	Calcium (CaO)
5	Unpigmented distal part of i1 (white)	42.191	0.276	Oxygen
		21.426	0.231	Phosphorus (P2O5)
		36.384	0.267	Calcium (CaO)
6	Tip of a1 (VPg = reddish)	42.785	0.411	Oxygen
		1.910	0.124	Magnesium (MgO)
		4.508	0.160	Aluminum (Al2O3)
		17.978	0.279	Silicon (SiO2)
		0.622	0.108	Phosphorus (P2O5)
		27.795	0.328	Potassium (K2O)
		1.680	0.242	Calcium (CaO)
		1.838	0.345	Iron (FeO)
		0.885	0.128	Zinc (ZnO)
7	Tip of p4 (VPg = red-brown)	42.190	0.279	Oxygen
		0.705	0.095	Silicon (SiO2)
		20.839	0.227	Phosphorus (P2O5)
		36.266	0.267	Calcium (CaO)

Table 1. *Continued.*

Sample number*	Tooth (pigmentation type)	Weight %	σ, Weight %	Element (Formula)
8	m1 protoconid tip (VPg = red-brown)	41.581	0.335	Oxygen
		1.163	0.129	Sodium (Na2O)
		0.674	0.077	Aluminum (Al2O3)
		1.166	0.104	Silicon (SiO2)
		19.689	0.228	Phosphorus (P2O5)
		32.355	0.282	Calcium (CaO)
		1.091	0.181	Iron (FeO)
		2.283	0.332	Tungsten (WO3)
B: *B. fissidens* (ZIN 104925/1271, 'Borehole #103/19'); Fig. 1B				
1	Tip of metacone (VPg = reddish)	35.345	1.689	Oxygen
		10.689	1.187	Phosphorus (P2O5)
		53.965	1.755	Calcium (CaO)
2	Tip of metacone (VPg = reddish)	42.395	2.046	Oxygen
		21.746	1.717	Phosphorus (P2O5)
		35.859	1.977	Calcium (CaO)
3	Tip of metacone (VPg = reddish)	42.614	1.790	Oxygen
		22.089	1.518	PhosphorusP2O5
		35.297	1.713	CalciumCaO
4	Lingual part of the ridge of the hypoconal flange (VPg = pale reddish)	34.833	0.462	Oxygen
		9.887	0.295	Phosphorus (P2O5)
		55.280	0.482	Calcium (CaO)
5	Lingual part of the ridge of the hypoconal flange (VPg = pale reddish)	40.620	2.938	Oxygen
		18.962	2.420	Phosphorus (P2O5)
		40.418	2.888	Calcium (CaO)
6	Lingual part of the ridge of the hypoconal flange (VPg = pale reddish)	39.752	0.319	Oxygen
		17.600	0.250	Phosphorus (P2O5)
		42.648	0.321	Calcium (CaO)
C: *B. fissidens* (ZIN 104908/1236, Shamar/A); Fig. 1C				
1	Tip of left I1 (VPg = black)	29.199	0.390	Oxygen
		7.242	0.187	Phosphorus (P2O5)
		14.548	0.237	Calcium (CaO)
		49.011	0.443	Iron (FeO)
2	Tip of left I1 (VPg = black)	30.227	0.384	Oxygen
		0.949	0.102	Silicon (SiO2)
		7.636	0.189	Phosphorus (P2O5)
		15.574	0.237	Calcium (CaO)
		45.613	0.435	Iron (FeO)

Table 1. *Continued.*

Sample number*	Tooth (pigmentation type)	Weight %	σ, Weight %	Element (Formula)
3	Tip of left I1 (VPg = black)	25.702	1.752	Oxygen
		2.973	0.499	Phosphorus (P2O5)
		12.695	0.932	Calcium (CaO)
		58.630	1.940	Iron (FeO)
4	The unpigmented distal part of the I1 apex (white)	31.872	1.304	Oxygen
		5.242	0.659	Phosphorus (P2O5)
		62.886	1.355	Calcium (CaO)
D: *B. fissidens* (GIN 664/201, Razdol'e); Fig. 1D				
1	Tip of m1 protoconid (PPt)	42.971	0.372	Oxygen
		22.649	0.315	Phosphorus (P2O5)
		34.381	0.356	Calcium (CaO)
2	Tip of m1 protoconid (PPt)	42.159	0.377	Oxygen
		1.473	0.197	Sodium (Na2O)
		21.461	0.308	Phosphorus (P2O5)
		34.907	0.357	Calcium (CaO)
3	Tip of m1 hypoconid (PPt)	42.284	0.443	Oxygen
		1.464	0.218	Sodium (Na2O)
		21.655	0.365	Phosphorus (P2O5)
		34.597	0.420	Calcium (CaO)
E: *B. fissidens* (ZIN 104903/1292, Korotoyak 2); Fig. 1E				
1	Tip of right I1 (PPt)	49.742	1.000	Oxygen
		12.434	0.590	Aluminum (Al2O3)
		19.641	0.738	Silicon (SiO2)
		10.142	0.722	Phosphorus (P2O5)
		8.041	0.585	Calcium (CaO)
2	Tip of right I1 (PPt)	42.807	0.937	Oxygen
		12.300	0.580	Silicon (SiO2)
		18.489	0.738	Phosphorus (P2O5)
		12.323	0.560	Calcium (CaO)
		14.081	0.839	Bromine
3	Tip of right I1 (PPt)	42.574	0.692	Oxygen
		1.887	0.282	Sodium (Na2O)
		11.167	0.377	Aluminum (Al2O3)
		18.326	0.487	Silicon (SiO2)
		3.720	0.366	Phosphorus (P2O5)
		5.442	0.379	Chlorine
		2.243	0.317	Potassium (K2O)
		14.641	0.504	Calcium (CaO)

Table 1. *Continued.*

Sample number*	Tooth (pigmentation type)	Weight %	σ, Weight %	Element (Formula)
4	Tip of right I1 (PPt)	48.849	1.202	Oxygen
		4.077	0.881	Sodium (Na2O)
		5.364	0.565	Aluminum (Al2O3)
		9.151	0.656	Silicon (SiO2)
		21.563	0.924	Phosphorus (P2O5)
		10.995	0.669	Calcium (CaO)

Note: * — number corresponds to orange point in Figs. 1 and 2.

dish (i1–m3 of *B. minor*, ZIN 104894, Bural-Obo/C; M1 of *B. fissidens*, ZIN 104925/1271, 'Borehole #103/19') to dark reddish-brown (I1 of *B. fissidens*, ZIN104908/1236, Shamar/A) (Fig. 1: A–C) and a fuzzy pigment pattern (PPt) that was typically situated on the teeth crowns and represented by pale patina-like patterns (m1–m2 of *B. fissidens*, GIN 664/201, Razdol'e; and I1, ZIN104903/1292, Korotoyak 2) (Fig. 1: D–E). The PPt of the last remains is attributed to the chemical leaching of the actual/true pigment during fossilization, although traces of the pigmented and unpigmented enamel border are retained, which may have occurred due to the replacement of ferruginous pigments with other substances. This assumption is partially confirmed by the comparative EDX analysis of several fossil teeth of *Beremendia* and some recent taxa (Fig. 2). The EDX analysis reveals the possibility of chemical leaching of the true pigment depending on burial conditions. The analyses show an absence of iron in different parts of the tooth crowns with PPt (Table 1).

The pigmented parts of the teeth crown i1–m1 of *B. minor* contain iron from 1.0±0.1% in protoconid enamel to 25.9±0.4% in incisor tip enamel (Table 1: A). The second specimen with more significant iron content is the first upper incisor of *B. fissidens* (ZIN 104908/1236), which display values from 45.6±0.4% to 58.6±1.9% (Table 1: C). These values were significantly higher in extant species, such as *S. isodon* (3.2±0.2–10.7±1.3%; Table 2: A) and *B. brevicauda* (1.0±0.5–8.0±3.9%; Table 3: A). There is a different combination of other chemical elements present in pigmented and unpigmented parts of crown enamel. The comparison between the same parts of *B. minor* (samples 1 and 8, Table 1: A) and *S. isodon* (samples 3 and 5, Table 2: A) reveals approximately equal values of phosphorus and calcium. The phosphorus and calcium content values (Table 1: D) in the m1 protoconid tip of *B. fissidens* (GIN 664/201) were approximately equal to the values of *B. minor* (sample 8, Table 1: A) and *S. isodon* (sample 3, Table 2: A). In contrast, the phosphorus and calcium content values (Table 1: E) in the first upper incisor enamel of *B. fissidens* (ZIN 104903/1292) were significantly lower than those of *B. minor* and *S. isodon*, probably because of the specific burial conditions of Korotoyak 2 locality. The burial-related change of the chemical content of the enamel pigment retains pigment patterns on the crown without pigment, i.e., ferruginous pigment fully leached together with changes of the other elements (phosphorus and calcium). The first upper incisor of *B. fissidens* (ZIN 104908/1236) also displays relatively low values of phosphorus and calcium content (Table 1: C) but does display content of iron. Thus, the specific burial conditions of Shamar A locality determined changes in pigment elemental content without iron leaching. The visible pigment areas of the first upper molar of *B. fissidens* (ZIN 104925/1271) display fully leached iron (Table 1: B) and significant upward shifting of the calcium content values (see samples 1, 4). The extant species without pigmented enamel, *C. shantungensis* and *A. squamipes*, display high values of calcium (Table 2: B, C) and low values of phosphorus in some cases (samples 2 and 3, Table 2: B).

DISCUSSION

General remarks. The EDX analysis of the visible pigment area and pigment pattern area of fossil shrew teeth reveals the very high iron content value in the

Table 2. Results of the EDX elemental analyses of the teeth of extant shrews.

Sample number	Tooth (pigmentation type)	Weight %	σ, Weight %	Element (Formula)
	A: *Sorex isodon* (201/A86) Fig. 2A			
1	Tip of a1 (VPg = red-brown)	40.539	0.280	Oxygen
		1.125	0.111	Sodium (Na2O)
		19.848	0.208	Phosphorus (P2O5)
		1.229	0.094	Potassium (K2O)
		31.868	0.250	Calcium (CaO)
		5.391	0.246	Iron (FeO)
2	Tip of p4 (VPg = red-brown)	40.498	0.324	Oxygen
		20.132	0.242	Phosphorus (P2O5)
		1.158	0.108	Potassium (K2O)
		29.434	0.279	Calcium (CaO)
		8.777	0.318	Iron (FeO)
3	Tip of m1 protoconid (VPg = red-brown)	41.668	0.315	Oxygen
		1.298	0.151	Sodium (Na2O)
		21.269	0.242	Phosphorus (P2O5)
		0.794	0.098	Potassium (K2O)
		31.674	0.281	Calcium (CaO)
		3.297	0.246	Iron (FeO)
4	Tip of i1 (VPg = dark brown)	44.651	4.056	Oxygen
		23.630	3.387	Aluminum (Al2O3)
		12.300	2.783	Phosphorus (P2O5)
		19.419	3.239	Calcium (CaO)
5	Tip of the 3rd denticle of i1 (VPg = red-brown)	39.625	1.233	Oxygen
		18.756	0.895	Phosphorus (P2O5)
		30.898	1.070	Calcium (CaO)
		10.722	1.311	Iron (FeO)
6	Tip of the 2nd denticle of i1 (VPg = red-brown)	40.341	0.405	Oxygen
		19.800	0.291	Phosphorus (P2O5)
		0.873	0.120	Potassium (K2O)
		30.989	0.350	Calcium (CaO)
		6.388	0.350	Iron (FeO)
		1.609	0.302	Zinc (ZnO)
7	Unpigmented part of i1 (white)	41.770	0.267	Oxygen
		1.163	0.116	Sodium (Na2O)
		20.832	0.218	Phosphorus (P2O5)
		36.235	0.257	Calcium (CaO)

Table 2. *Continued*.

Sample number	Tooth (pigmentation type)	Weight %	σ, Weight %	Element (Formula)
B: *Crocidura shantungensis* (ZIN 89478) Fig. 2B				
1	Tip of i1 (white)	39.986	0.280	Oxygen
		17.967	0.221	Phosphorus (P2O5)
		42.048	0.281	Calcium (CaO)
2	The distal part of i1 (white)	37.788	5.145	Oxygen
		14.521	4.122	Phosphorus (P2O5)
		47.690	5.189	Calcium (CaO)
3	Distal part of i1 (white)	35.090	0.675	Oxygen
		10.289	0.440	Phosphorus (P2O5)
		54.621	0.703	Calcium (CaO)
4	Tip of p4 (white)	39.563	4.726	Oxygen
		17.304	3.924	Phosphorus (P2O5)
		43.133	4.652	Calcium (CaO)
5	Tip of m1 protoconid (white)	43.396	6.921	Oxygen
		23.316	5.593	Phosphorus (P2O5)
		33.288	6.931	Calcium (CaO)
6	Tip of m1 hypoconid (white)	40.720	5.424	Oxygen
		19.119	4.332	Phosphorus (P2O5)
		40.161	5.418	Calcium (CaO)
C: *Anourosorex squamipes* (ZIN 38946) Fig. 2C				
1	Tip of i1 (white)	40.954	0.271	Oxygen
		19.487	0.221	Phosphorus (P2O5)
		39.559	0.268	Calcium (CaO)
2	Distal part of i1 (white)	40.950	0.253	Oxygen
		19.480	0.205	Phosphorus (P2O5)
		39.569	0.251	Calcium (CaO)
3	Distal part of i1 (white)	41.132	0.250	Oxygen
		0.947	0.103	Sodium (Na2O)
		20.065	0.201	Phosphorus (P2O5)
		0.549	0.078	Chlorine
		37.307	0.242	Calcium (CaO)
4	Tip of a1 (white)	39.558	4.342	Oxygen
		17.297	3.694	Phosphorus (P2O5)
		43.145	4.226	Calcium (CaO)
5	Tip of p4 (white)	39.093	6.135	Oxygen
		16.567	4.992	Phosphorus (P2O5)
		44.341	6.106	Calcium (CaO)

Table 3. Results of the EDX elemental analyses of the teeth of fossil *Sorex* and *Dolinasorex* from Early Pleistocene Gran Dolina site (Atapuerca, Burgos, Spain) and extant *Blarina*

Sample number	Tooth (pigmentation type)	Weight %	σ, Weight %	Element (Formula)
	A: *Blarina brevicauda* (by Dumont et al. 2014: table 1)			
	Apex of the first upper incisor	2.3	1.2	Carbon
	(pigmented enamel, Pe)	36.4	4.2	Oxygen
		2.0	0.2	Sodium
		1.9	0.2	Silicon
		16.7	2.7	Phosphorus
		32.7	3.9	Calcium
		8.0	3.9	Iron
	Apex of the first upper incisor	3.7	1.2	Carbon
	(unpigmented enamel, Ue)	38.8	1.8	Oxygen
		1.2	0.3	Sodium
		1.1	0.2	Silicon
		18.7	0.8	Phosphorus
		35.5	1.4	Calcium
		1.0	0.5	Iron
	B: *Sorex* (by Moya-Costa et al. 2018: table 2)			
8a	Tip of the first lower incisor	38.98	–	Phosphorus
	(outer layer of enamel)	60.64	–	Calcium
		0.38	–	Iron
3li	Cutting edge of first lower incisor	37.11	–	Phosphorus
	(outer layer of enamel)	61.12	–	Calcium
		1.27	–	Iron
5la	Lower part of first lower incisor	34.97	–	Phosphorus
	(outer layer of enamel)	56.47	–	Calcium
		8.56	–	Iron
	C: *Dolinasorex glyphodon* (by Moya-Costa et al. 2018: table 4)			
1	Tip of the first lower incisor	24.25	–	Phosphorus
	(outer layer of enamel)	71.05	–	Calcium
		4.71	–	Iron
2	Tip of the first lower incisor	25.57	–	Phosphorus
	(outer layer of enamel)	56.95	–	Calcium
		17.48	–	Iron

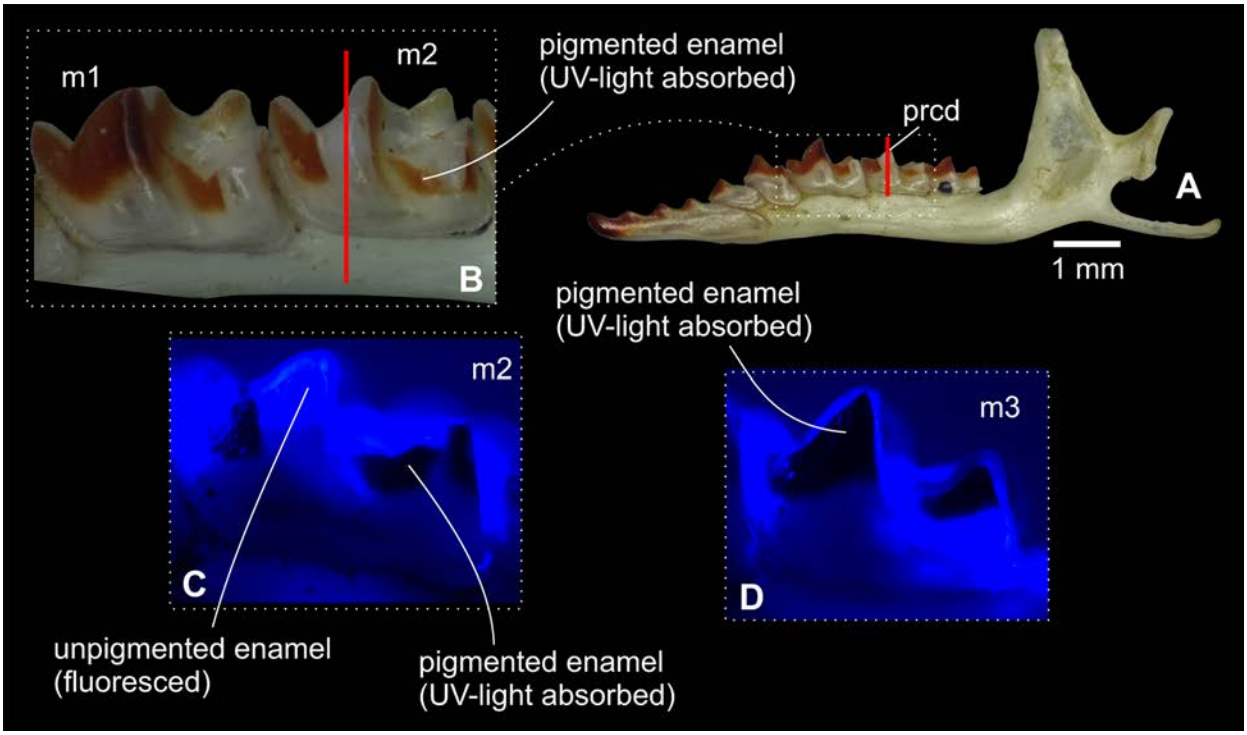

Fig. 3. *Sorex minutus* dentary (A), lower teeth of ZIN 92951(B–D): **(A)** The left dentary (ZIN 92951), optic photograph, lateral view; **(B)** The left m1 and m2 with differential pigmentation, optic photograph, tilted lateral view; **(C)** The left m2 with unpigmented belt in transmitted UV-light, fluorescent photograph, lateral view; **(D)** The left m3 with regular pigmentation, fluorescent photograph, lateral view. Scale bar represent 1 mm **(A)**, **B**–**D** unscaled. Abbreviations: prcd – protoconid.

teeth enamel of *Beremendia* species (up to 58.6%) compared to extant species, *S. isodon* (up to 12%) and *B. brevicauda* (up to 11.9% by Dumont et al. 2014; and up to 12.29% by Strait and Smith 2006). The observed differences between the maximal value of *B. minor* (25.9%) and *B. fissidens* (58.6%) cannot be considered interspecific features. The determination of specific parameters of the pigment elemental composition requires additional mass comparison. The analysis of the other elements, phosphorus and calcium, reveals value similarity between fossil specimens of *B. minor* with VPg (ZIN 104894) and extant specimens of *S. isodon*. This fact suggests chemically neutral burial conditions in Bural-Obo locality, where the whole right dentary of *B. minor* was found with the retained natural colour of the bone and teeth, including pigmented areas (Fig. 1A). The EDX analysis of this specimen teeth confirmed the stability and "permanency" of the pigment content compared with recent species. On the other hand, the similarity of the content values of phosphorus and calcium between *S. isodon/B. minor* and the specimen of *B. fissidens* with PPt (GIN 664/201) cannot point to chemically neutral burial conditions in Razdol'e locality because the iron was fully leached from the teeth of this specimen. Two other specimens of *B. fissidens*, ZIN 104925/1271 with VPg and ZIN 104903/1292 with PPt, show a significant shifting of the content values of phosphorus and calcium with loss of iron. The visible pigment areas without iron on the first upper tooth from the Troitskoye vicinity (ZIN 104925/1271) attract our attention as an instance of disparity between visibility and enamel content.

The EDX analysis confirmed the absence of iron in the tooth enamel of *A. squamipes* as well as in the enamel of *C. shantungensis* (Table 2: B and C). In addition, we revealed similarity in phosphorus and calcium values between white-toothed shrews and some fossil teeth of *B. fissidens* (ZIN 104925/1271 and ZIN 104903/1292). This fact restricts the possible usage of EDX results of the enamel analyses of

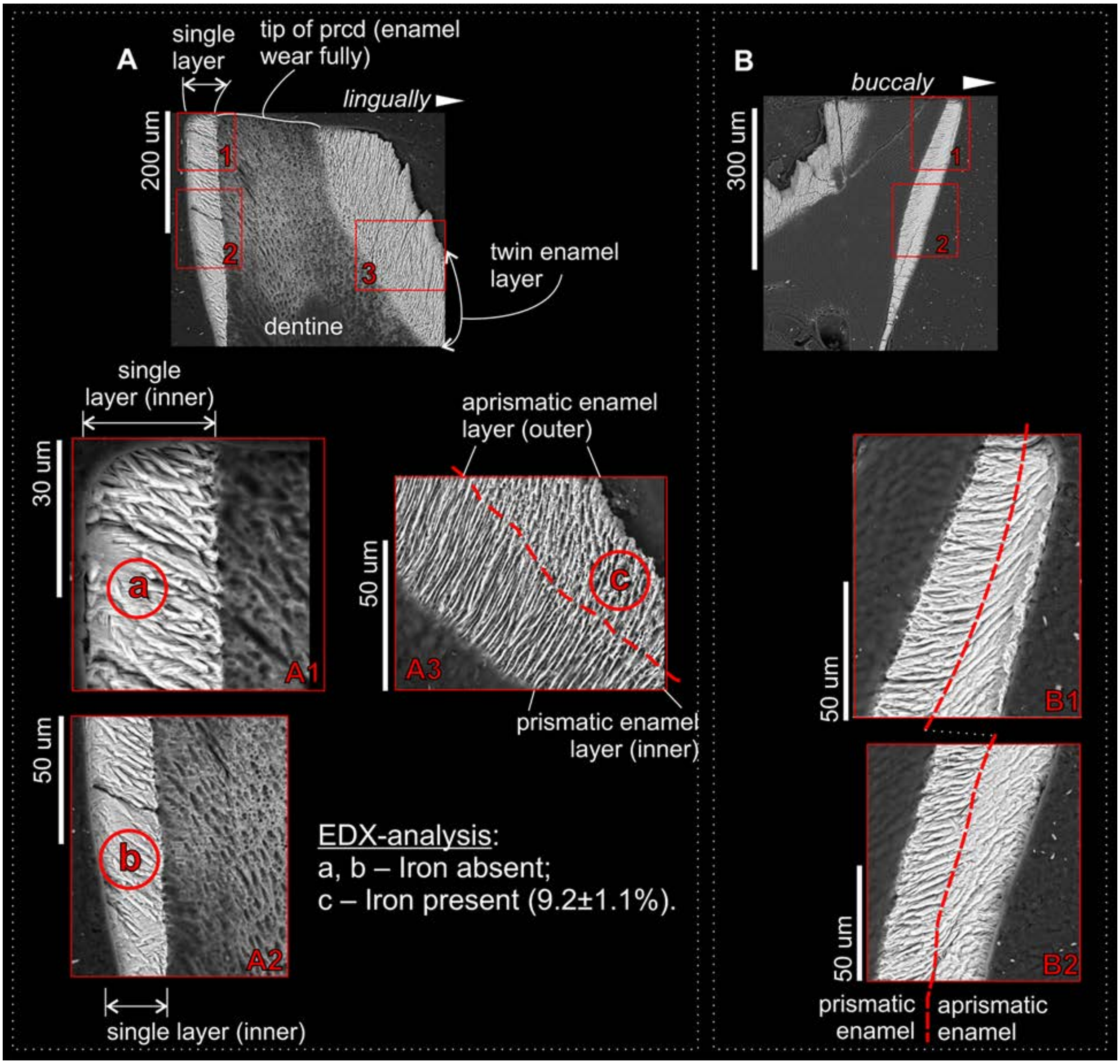

Fig. 4. *Sorex minutus* SEM-images of m2 transversal section: **(A)** SEM-image of protoconid of the left m2 of ZIN 92951 with magnifications **(A1–A3)**; **(B)** SEM-image of protoconid of the left m2 (unpigmented belt area) of ZIN 84531 (regular pigmentation) with magnifications **(B1–B2)**. Scale bars in microns. Abbreviations: a–c – EDX-samples.

white-toothed shrews for directly proving that iron is absent in fossil teeth.

Moya-Costa et al. (2018) published structural analysis and tooth enamel composition of quaternary shrews, *Sorex* indet. and *Dolinasorex glyphodon* Rofes et Cuenca-Bescos, 2009, from the Gran Dolina site (Atapuerca, Burgos, Spain). We partly used the results of the authors to compare with our results. Because the authors acquired the elemental values from several layers of enamel, we used their values from outer layers for correct comparisons (Table 3: B and C). The comparison shows a significant shift in phosphorus and calcium values in specimens from the Gran Dolina site. The iron content broadly varies among 0.04–22.17% in *Sorex* and 1.42–26.27% in *D. glyphodon* (Moya-Costa et al. 2018: tables 2 and 4). The iron value of the first lower incisor of *D. glyphodon* is approximately the same as the value of i1 of *B. minor* (ZIN 104894).

UV detection of the tooth pigment. The UV method was described by Patterson and McGrew (1937). The authors specified that under UV light, the coloured part of teeth of *Blarina* did not fluoresce, but the unpigmented part fluoresced in a bluish colour. We performed UV detection of tooth pigment in *Shargainosorex angustirostris* Zazhigin et Voyta, 2018 and compared it to *Sorex daphaenodon* (Zazhigin and Voyta 2018). The specific methodology of UV detection was not discussed in this article due to the its simplicity. However, the current investigation suggests restricted applicability of the UV method for fossil taxa. This conclusion is based on observation of the rare case of "differential pigmentation" in *S. minutus* (ZIN 92951) from Kandalaksha Nature Reserve (Murmanskaya Oblast, Karelia Region, Russia; collected by Nadezhda S. Boyko in 1999). The specimen bore normal pigmentation on all upper teeth as well as the lower incisor, a1, p4 and m3, but an abnormal pigment of lower m1 and m2 of both dentaries. The hypoconid of m1 has a wide vertical fully unpigmented belt; the protoconid with the posterior part of paracristid of m2 has a similar unpigmented belt, and the hypoconid has a local unpigmented area on the tip (Fig. 3A). Therefore, the differential pigmentation is represented by the unpigmented belt of m1–m2 and displays non-selectivity using the UV method. UV light is absorbed by the pigmented part of *S. minutus* teeth and fluoresced on the belts (Fig. 3B). In the case of diagenetic (or post-burial) pigmentation of the fossil teeth (e.g., white-toothed shrew), the UV method detects "pigment", and vice versa: the unpigmented belt or area (for instance, red-toothed shrew *Nesiotites*, see Furió and Pons-Monjo 2013) represents as unpigmented.

Twin enamel layer and pigmentation. Dötsch and Koenigswald (1978: 68) wrote: "In *Sorex* [...], iron can only be detected in the outermost prism-free layer, which is also macroscopically coloured red", and further "The soricids have a prismatic enamel under the pigmented (prism-less) enamel [...]". Thus, the pigmented enamel layer displays an aprismatic structure and lays outward of the inner unpigmented prismatic enamel layer. Our analysis of the enamel microstructure of the unpigmented belt of the m2 protoconid of *S. minutus* (ZIN 92951) compared to the *S. minutus* specimen (ZIN 84531) with regular pigmentation of lower teeth reveals the loss of the aprismatic outer layer within the unpigmented belt. The enamel microstructure of the aberrant tooth (ZIN 92951) differs from the microstructure of the common tooth (ZIN 84531) in the presence of the single prismatic enamel layer on the buccal side (the belt situated) instead of the twin layer (Fig. 4: A1, A2), and the twin layer is on the lingual side of the protoconid (Fig. 4: A3). In contrast, the tooth with a regular pigmentation shows a twin layer on the buccal side (Fig. 4: B1, B2). EDX analysis reveals the presence of iron in the aprismatic enamel on the lingual side of the aberrant m2 (the iron content value is 9.2±1.1%; Fig. 4, sample c) but the absence of iron in the prismatic layer of the belt (Fig. 4, see samples a and b). Therefore, the ferruginous pigment is closely connected with the outer enamel, as previously stated by Dötsch and Koenigswald (1978) and Dumont et al. (2014). However, the question posed by Dötsch and Koenigswald (1978: 69) remains: "[...] whether the pigmentation of the enamel is generally bound to "prism-less" enamel, or whether this convergence is coincidental".

CONCLUSIONS

The pigment of tooth enamel is an important odontological character character for assessing soricid taxonomy and phylogeny (Repenning 1967; Dannelid 1998). Two methods for pigment determination are known: the UV method and EDX analysis. Our study revealed that the UV method did not distinguish between truely pigmented parts of the soricine tooth crown and diagenetic burial-related pigmentation; i.e., the natural ferruginous tooth pigment and the diagenetically added pigment, which are formed by chemical substitution, absorbed UV light equally well. Thus, the applicability of the UV detection of tooth pigment must be revised and most likely is not effective for fossil taxa. EDX analysis is more precise than the former and can be used for the detection of iron in extant and fossil taxa. However, additional studies are required to determine the limitations of the method in relation to fossil specimens. Our results reveal the case of chemically neutral burial conditions in Bural-Obo locality, where EDX analysis confirmed the stability and "permanency" of a pigment content of *B. minor* compared to the recent species, *S. isodon.* Another result showed a significant shift in the content values of phosphorus and calcium together with lost iron (ZIN 104925/1271, ZIN 104903/1292). In addition, the former specimen displays visible pigment. Therefore, visible pigmentation did not always indicate the presence of ferruginous pigment. The cases of “pigmented teeth” of *M. desnoyersianus* (Engesser 2009; the presence of VPg) or “iron absence” in this taxon (Klietmann et al. 2013; made EDX analysis) neither proves nor refutes the presence of ferruginous pigment. However, this question is significant for the phylogeny of *Miosorex* s. lato.

EDX analysis confirms the complete absence of ferruginous pigmentation in *Anourosorex* dentition and is comparable to *Crocidura's* content of phosphorus and calcium. These values are significantly different from those shown by *S. isodon* and *Beremendia* (from Bural-Obo/C).

Furió and Pons-Monjo (2013) used the term “differential pigmentation” to explain the irregular pigmentation on the fossil teeth of *Nesiotites*. Our analysis of the fossil and recent specimens reveals different reasons for differential pigmentation formation. The first reason is related to fossilization, namely, the chemical alterations of the buried specimen. In the different cases, unicolour teeth, teeth with VPg and teeth with PPt were found. We supposed that the visible ‘pigment pattern’ is a reflection of the twice-layered enamel (Fig. 4B). The optic effect of PPt is likely connected with some structural character of the outer layer; as a result, we can see pigment “without” pigment (Fig. 1B). In addition, the local chemical micro conditions can form VPg and PPt while one tooth-row (e.g., *Nesiotites* on fig. 2:2, by Furió and Pons-Monjo 2013). The second reason is related to a developmental disorder, namely, the enamel organ disorder, which locally stops forming the twin enamel layer (Figs. 3, 4). Thus, the number of enamel layers of *Anourosorex* is a significant question.

Our results and published data of EDX analysis of the elemental content and SEM-image analysis of enamel microstructure after Dötsch and Koenigswald (1978) again raise the question of a relationship between ferruginous pigmentation and enamel microstructure. Is there any structural difference between the outer enamel of red-toothed and white-toothed shrews?

ACKNOWLEDGEMENT

This study was completed within the framework of the Federal themes of the Zoological Institute no. AAAA-A19-119032590102-7 “Phylogeny, morphology, and systematics of placental mammals,” and Geological Institute “Paleontological grounds for the stratigraphic scale of the upper Cenozoic of Northern Eurasia.” In the study partly used the collection materials of the Zoological Institute of RAS (http://www.ckp-rf.ru/usu/73561/). This study was partly funded by Project no. 19-04-00049 of the Russian Foundation for Basic Research and the Program of the Russian Academy of Sciences Presidium and Ministry of Education and Science of Russia “Evolution of the organic world. The role and significance of planetary processes”. Authors are grateful to Mikhail P. Zhurbenko, Anna A.Kijashko, and Evgenii S. Popov (all Botanic Institute of Russian Academy of Sciences, St. Petersburg, Russia) for organizing the tooth pigmentation investigations using UV method.

REFERENCES

Agadjanian A.K. 2009. The Pliocene-Pleistocene small mammals of the Russian Plain. Izdatel'stvo Nauka, Moscow, 676 p. [In Russian].

Dannelid E. 1998. Dental adaptations in shrew. In: J.M. Wójcik and M. Wolsan (Eds.). Evolution of Shrews. Mammal Research Institute Polish Academy of Sciences, Białowieża: 157–174.

Devjatkin E.V. and Zazhigin V.S. 1974. Eopleistocene deposits and new localities of mammal fauna from Northern Mongolia. In: N.N. Kramarenko (Ed.). Fauna i biostratigraphia mezozoya i kainozoya Mongolii. Izdatel'stvo Nauka, Moscow: 357–363. [In Russian].

Devjatkin E.V., Zazhigin V.S. and Maleeva E.M. 1982. The new late Pliocene localities of small mammals' fauna of the Northern Mongolia. In: K.V. Nikiforova (Ed.). Stratigraphy and Paleogeography of the Antropogene. Izdatel'stvo Nauka, Moscow: 100–114. [In Russian].

Doben-Florin U. 1964. Die Spitzmäuse aus dem Altburdigaliumvon Wintershof-West bei Eichstätt in Bayern. *Abhandlungender Bayerischen Akademie der Wissenschaften, mathematisch-naturwissenschaftliche Klasse (Neue Folge)*, **117**: 1–82.

Dötsch C. and Koenigswald W. 1978. Zur Rotfärbung von Soricidenzähnen. *Sonderdruck aus Z. f. Säugetierkunde*, **43**(2): 65–70.

Dumont M., Tütken T., Kostka A., Duarte M.J. and Borodin S. 2014. Structural and functional characterization of enamel pigmentation in shrew. *Journal of Structural Biology*, **186**: 38–48. https://doi.org/10.1016/j.jsb.2014.02.006

Engesser B. 2009. The Insectivores (Mammalia) from Sansan (Middle Miocene south-western France). *Schweizerische Paläontologische Abhandlungen*, **128**: 1–91.

Furió M. and Pons-Monjo G. 2013. The use of the species concept in paleontology. Comment on "*Nesiotites rafelinensis* sp. nov., the earliest shrew (Mammalia, Soricidae) from the Balearic Islands, Spain" by Rofes et al., 2012. *Palaeontologia Electronica*, **16.2.16A 16**: 1–7. https://doi.org/10.26879/336

Janis C.M. and Fortelius M. 1988. On the means whereby mammals achieve increased functional durability of their dentitions, with special reference to limiting factors. *Biological Review*, **63**: 197–230.

Jernvall J. 1995. Mammalian molar cusp patterns: Developmental mechanism of diversity. *Acta Zoologica Fennica*, **198**: 1–61.

Klietmann J., Nagel D., Rummel M. and Van den Hoek Ostende L.W. 2013. Tiny teeth of consequence: vestigial antemolars provide key to Early Miocene soricid taxonomy (Eulipotyphla: Soricidae). *Comptes Rendus Palevol*, **12**: 257–267. https://doi.org/10.1016/j.crpv.2013.05.008

Lopatin A.V. 2002. The Earliest Shrew (Soricidae, Mammalia) from the Middle Eocene of Mongolia. *Paleontological Journal*, **36**: 650–659.

Moya-Costa R., Cuenca-Bescós G., Bauluz B. and Rofes J. 2018. Structure and composition of tooth enamel in quaternary soricines (Mammalia). *Quaternary International,* **481**: 52–60. https://doi.org/10.1016/j.quaint.2017.04.039

Patterson B. and McGrew P.O. 1937. A soricid and two erinaceids from the White River Oligocene. *Geological Series of Field Museum of Natural History*, **6**: 245–272.

Repenning C.A. 1967. Subfamilies and genera of the Soricidae. Classification, historical zoogeography and temporal correlation of the shrews. *United States Survey Professional Paper*, **565**: 1–74.

Reumer J.W.F. 1994. Phylogeny and distribution of the Crocidosoricinae (Mammalia: Soricidae). In: J.F. Merrit, G.L. Kirkland and R.K. Rose (Eds.). Advances in the biology of shrews, Special Publication 18. Carnegie Museum of Natural History, Pittsburgh: 345–356.

Rofes J., Bover P., Cuenca-Bescós G. and Alcover J.A. 2012. *Nesiotites rafelinensis* sp. nov., the earliest shrew (Mammalia, Soricidae) from the Balearic Islands, Spain. *Palaeontologia Electronica,* **8A 15**: 1–12. https://doi.org/10.26879/282

Strait S.G. and Smith S.C. 2006. Elemental analysis of soricine enamel: pigmentation variation and distribution in molars of *Blarina brevicauda*. *Journal of Mammalogy*, **87**: 700–705. https://doi.org/10.1644/05-MAMM-A-265R4.1

Vasilyan D., Zazhigin V.S. and Böhme M. 2017. Neogene amphibians and reptiles (Caudata, Anura, Gekkota, Lacertilia, and Testudines) from the south of Western Siberia, Russia, and Northeastern Kazakhstan. *PeerJ*, **5**: 1–65. https://doi.org/10.7717/peerj.3025

Zazhigin V.S. 1980. The rodents of late Pliocene and Antropogene in the Southern West Siberia. Isdatel'stvo Nauka, Moscow, 339 p. [In Russian].

Zazhigin V.S. 1989. Upper Pliocene reference sections and their biostratigraphic characteristic (based on mammals). In: N.A. Logachev (Ed.). Late Cenozoic of Mongolia (stratigraphy and paleogeography). Izdatel'stvo Nauka, Moscow: 10–24. [In Russian].

Zazhigin V.S. and Voyta L.L. 2019. North Asian Pliocene-Pleistocene beremendiin shrews (Lipotyphla: Soricidae): A description of material from Russia (Siberia), Kazakhstan, and Mongolia and the paleobiology of *Beremendia*. *Journal of Paleontology*, ***in press***. https://doi.org/10.1017/jpa.2019.51

Ziegler R. 1989. Heterosoricidae und Soricidae (Insectivora, Mammalia) aus dem Oberoligozän und Untermiozän Süddeutschlands. *Stuttgarter Beiträge zur Naturkunde*, **154**: 1–73.

Submitted July 22, 2019; accepted September 6, 2019.